Computer Methods in Biomechanics and Biomedical Engineering, Vol. 4, pp. 127–148
Reprints available directly from the publisher
Photocopying permitted by license only

A Biomechanical Model of the Upper Airways for Simulating Laryngoscopy

M. A. F. RODRIGUES[a], D. GILLIES[a,*] and P. CHARTERS[b]

[a]*Department of Computing, Imperial College of Science, Technology and Medicine, 180 Queen's Gate, London SW7 2BZ, United Kingdom;* [b]*Department of Anaesthesia, Walton Hospital, Rice Lane, Liverpool L9 1AR, United Kingdom*

(Received 5 December 1999; In final form 22 May 2000)

This paper describes a three-dimensional finite element model of the human upper airways during rigid laryngoscopy. In this procedure, an anaesthetist uses a rigid blade to displace and compress the tongue of the patient, and then inserts a tube into the larynx to allow controlled ventilation of the lungs during an operation. A realistic model of the main biomechanical aspects involved would help anaesthetists in training and in predicting difficult cases in advance. For this purpose, the finite element method was used to model structures such as the tongue, ligaments, larynx, vocal cords, bony landmarks, laryngoscope blade, and their inter-relationships, based on data extracted from X-ray, MRI, and photographic records. The model has been used to investigate how the tongue tissue behaves in response to the insertion of the laryngoscope blade, when it is subjected to a variety of loading conditions. In particular, the mechanical behaviour of the soft tissue of the tongue was simulated, from simple linear elastic material to complex non-linear viscoelastic material. The results show that, within a specific set of tongue material parameters, the simulated outcome can be successfully related to the view of the vocal cords achieved during real laryngoscopies on normal subjects, and on artificially induced difficult laryngoscopy, created by extending the upper incisors teeth experimentally.

Keywords: Deformable models; Simulation; Upper airways; Laryngoscopy

1. INTRODUCTION

Laryngoscopy is a procedure, carried out by anaesthetists, in which the tongue of a patient is compressed and displaced to one side of the mouth using a rigid blade. A tube is subsequently inserted into the larynx to feed a mixture of oxygen and anaesthetic gas to the lungs. The procedure is not without difficulty or danger, and it would be highly desirable to predict which patients could be at risk, before the procedure is started. Difficult intubation can cause mortality associated with anaesthesia, but yet the reasons for difficult laryngoscopy have not been completely identified or explained.

*Corresponding author.

Early investigators concentrated on measurement techniques of skeletal structures of the mouth [5] and neck [49], and on geometric methods of analysing laryngoscope blade shapes [25]. A variety of such variables have been associated with unexpectedly difficult laryngoscopy, such as, anatomical factors, the laryngoscope used, and the technique of laryngoscopy. Other factors such as the experience of the person intubating and the degree of muscle relaxation may influence laryngoscopic measurements. In contrast to studies of geometric factors, the contribution of soft tissues was initially neglected. However, the importance of the tongue in particular has now been recognised [9, 45]. In fact, the tongue is the main obstacle to a direct view of the larynx, and thus, an accurate representation of its behaviour plays a key role in any simulation model of rigid laryngoscopy.

The human tongue is a very complex structure, composed of layers of different muscles, that behave in a non-linear viscoelastic way. A practical problem is the acquisition of parameters for modelling the tissue of the tongue. Recently, the elastic properties of biological soft tissues have become the subject of increasing research efforts [35]. However, most studies are based on cadavars and very little useful data has become available. Most studies inappropriately apply the cadaver data to living subjects.

It is the main purpose of this work to use a biomechanical model based on clinical measurements during laryngoscopy to investigate the behaviour of the tongue under a set of different loading conditions. As far as we know, this is the first attempt to create a realistic three-dimensional laryngoscopy model based on real data extracted from patients.

1.1. Previous Tongue Models

The human tongue has previously been modelled for computer graphics applications, such as speech production and facial animation. Little can be gained from the work on facial animation since, in cases where the tongue has been modelled at all, it is over simplified, for example as a paralleliped with rudimentary movements [23, 8]. In the context of speech production, however, the modelling of the tongue has often played an important part.

Examples of pioneering researchers modelling the tongue during speech are Mermelstein and Perkel [27, 37]. Specifically, Mermelstein proposed a model consisting of a slow-moving spherical body which supports a fast-moving flexible tip. Perkell reported on a computational simulation of the tongue as a two-dimensional lumped-constant elastic system. Both models are overly simple tongue representations. Other two-dimensional work at the very simple end are those reported in [11, 17, 20].

Motivated by the work of Perkell, however, Kiritani *et al.*, have modelled the tongue as a linear elastic body in three dimensions, by functionally dividing it into 14 tetrahedral elements [18]. Within each unit, very basic movements represent different muscle contraction effects on the tongue. This work is most closely related to ours in that it represents the tongue by a functional model composed of geometric elements in three dimensions. However, the complex structure of the tongue is represented by a very coarse mesh, with equally simplistic definition of boundary conditions and kinematics. In addition, the behaviour of the tongue is oversimplified in that it is linear elastic. This certainly is only valid for very small deformations and strain. Although the linear approach is extensively used in modelling, the visual result and behaviour of large deformation modelling using linear elasticity is seldom satisfactory.

Neither of these models have been backed up with a full validation study including medical data from speech experiments, such as those reported by Stone [50]. Stone proposed a three-dimensional functional model of the tongue by defining 5 segments in the lengthwise plane (one medial and 4 laterals), and 5 segments in the crosswise plane (root, posterior, dorsal, middle, and anterior). This model was a first step in describing sagittal

movement, coronal movement, and linguopalatal bracing for all phones in terms of segmental displacement and rotation of the tongue. To validate the model, Stone used ultrasound and MR images, electropalatography, and X-ray measurements. In our work, we also follow an experimental approach using MR and VHS images, X-rays, dental impressions, and photographic records to validate the tongue deformations obtained from different model configurations.

Similar to Stone's model, Pelachaud *et al.*, have proposed a tool to model tongue movement during speech production [36]. In particular, these authors retained only 3 segments in the lengthwise and crosswise tongue planes. Essentially, their kinematic tongue model consists of a mesh composed of 9 triangles that represent charge centres for an equi-potential surface field. Pelachaud *et al.*, specified a tongue shape for each vowel and consonant, using the results obtained in some studies which characterise tongue shape during speech production, particularly those of Stone. Even though there is no universal shape for each phonemic item, those shapes they established achieved realistic tongue behaviour.

These models simulate variations of the tongue shapes in response to deliberate movements. By contrast, as laryngoscopy is normally carried out under general anaesthesia, we need to simulate involuntary tongue deformations caused by blade contact. These deformations are difficult to predict because they depend on biomechanical parameters such as elastic tongue properties and contact forces.

1.2. Soft Tissue Modelling

Although many approaches have been proposed for soft tissue modelling, either in the field of computer graphics or in domains closer to biomechanics, only a few papers have been published on the realistic behaviour of soft tissue during deformation.

Modelling deformations of a patient's anatomy has traditionally been accomplished by using surface models. Examples are the work done on skin, with particular application to facial expression representations [39, 31, 34, 29]. A major problem with surface-based models is that they do not model the interior of the organ, and therefore, do not allow for volumetric behaviour. Hence, mass-spring models in three-dimensions and ellipsoid structures are anatomically more appropriate [56, 53, 47, 57]. These models account for a geometric structure which allows an interaction between bones, muscles, fatty tissue, and skin. The definition of the geometry of the organ in both approaches is generally done *ad-hoc*, and particularly in the mass-spring models, where there are difficulties in determining the optimal configuration of the spring network. Further, linear elasticity concepts are often used in these models as a way to represent the behaviour of the organ's deformation.

Recent research in the field of biomechanics has shown that a fairly realistic model for soft tissue has non-linear viscoelastic properties [12, 46]. Many non-linear finite element models have been developed for soft tissue simulation, mainly for the lungs [32, 55, 21] and the ventricles [16, 15, 7, 30, 51, 52]. Finite element models do not suffer from geometry problems, since the definition of the finite element mesh geometry leads to straightforward computation of element parameters [2]. Other examples in biomechanics include a surgical simulator using finite element analysis in which a realistic three-dimensional computer model of the eye and its surroundings is modelled with a complex behaviour [46]. This behaviour is represented by large non-linear incompressible Mooney–Rivlin [28] elastic deformations. Systems for computer-aided plastic surgery are also good realistic examples [53, 38, 19]. Specifically, Pieper *et al.*, developed an interactive graphics system for plastic surgery which accounts for the three-dimensional finite element structure and mechanical properties of human facial tissue [38]. Koch *et al.*, described a highly realistic three-dimensional system for simulating facial surgery using finite element models [19]. The work of Chen

and Zeltzer, in particular, is a novel finite element model of skeletal muscle that can be used both to simulate forces and to visualise the dynamics of muscle contraction [6]. Recently, Lee *et al.*, have integrated a realistic biomechanical simulation into facial modelling [22]. On the evidence of their own literature, the use of finite element analyses for the modelling of the behaviour of biological systems has proved an invaluable approach to represent realistic soft tissue deformations, and thus, has a significant part in soft tissue mechanics.

We have developed a three-dimensional finite element model of the upper airways for simulating laryngoscopy. A central issue in building such a model is to find a way to represent the behaviour of the tongue so that the relationship between mouth measurements, blade models, and different tongue deformations can be analysed. For this purpose, the finite element method was used to model structures such as the tongue, ligaments, larynx, vocal cords, bony landmarks, laryngoscope blade, and their inter-relationships, based on data extracted from X-ray, MRI, and photographic records. We have a special interest in the main anatomical factors leading to difficult laryngoscopy, particularly the behaviour of the tongue. Hence, the mechanical behaviour of the soft tissue of the tongue was simulated, from simple linear elastic material to complex non-linear viscoelastic material. To determine the set of model configurations that provide the most realistic behaviour, the simulation results were compared with actual measurements of the view of the vocal cords obtained from two different clinical experiments.

Section 2 reports on the two clinical experiments – a normal case and an artificially induced difficult case. These experiments provided data on the anatomy of the upper airways of the patient, and measurements of the view of the vocal cords achieved in each case. Section 3 describes our three-dimensional finite element model of the upper airways. A series of model simulations using the data provided by the normal case are performed in Section 4. In Section 5, we show that difficult laryngoscopy is also reproducible by applying the same analyses and tongue models utilised in the easy case. Section 6 shows some illustrative sequences of the deformations of the tongue obtained using the model. The final section presents the main conclusions, discusses the merits and limitations of the model, and gives directions for future work.

2. CLINICAL EXPERIMENTS

Two different laryngoscopic experiments were carried out on the same subject. In the first experiment, the anatomy of the subject on whom normal rigid laryngoscopy was carried out using a curved laryngoscope blade was used as the basis of our geometric model. In the second experiment, the anatomy of this normal subject was changed empirically by using a prosthesis attached to her upper incisors, so as to simulate a common difficult laryngoscopic situation, the patient with prominent maxillary incisors.

The empirical measurement of the view of the laryngeal inlet depends on the depth of insertion of a probe and the angle through which the probe turns to view all of the laryngeal inlet. The vocal cords view was used to find the best and the worst eye-line deviation values, as shown in Figure 1. In the best situation the probe is aligned with the

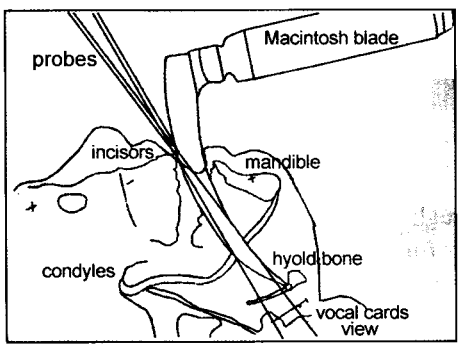

FIGURE 1 Laryngoscopic drawing of the subject illustrating the best and the worst views of the vocal cords. Lateral photos were used to obtain an outline that we could overlay on the X-rays and make other similar comparisons.

posterior part of the larynx and then it is rotated forward to record the maximum forward position. The length of larynx visible is the arc at the base of the triangle through which the probe has rotated, as represented in Figure 2. The blade contact with the upper incisors was taken by the anaesthetist as a reference point only, and in no instance was the blade rotated around the incisors.

In the normal laryngoscopic situation (Fig. 1), the patient had the probe inserted to a depth of 11.8 cm, as measured by the anaesthetist. The overlying probe images (the one when the probe is aligned with the posterior part of the larynx and the other when it is rotated forwards) gave the angle measured empirically between the two positions at the incisor point as 7°, as geometrically illustrated in Figure 2. According to this representation, the view is estimated as 1.4 cm. We adjust this lower value for the view by adding the width of one probe (0.2 cm) as an estimation of error, and then the corrected view can be estimated as 1.6 cm. Alternatively, this value can be calculated using the blade measurements as the reference. By mapping the blade measurements with those extracted from Figure 1, a very similar value of 1.65 cm is obtained.

The next situation to consider is the difficult case using a maxillary prosthesis. This was conducted by modifying the geometric mouth measurements. Using a prosthesis of 1.5 cm of thickness attached to the upper incisors of the patient, the upper incisors point is physically displaced forwards. The corresponding diagrams are shown in Figures 3(a) and 3(b). As measured along the probe, the distance from the tip of the prosthesis to the back of the larynx was 13.6 cm. In this situation, the space to accommodate the tongue is functionally reduced by alteration of one specific geometric parameter of the anatomy of the patient, and thus, the range of movement of the blade is reduced. The diagrams are adjusted to show the upper incisor point correctly positioned relative to the prosthesis. With this arrangement, the anaesthetist saw just the back of the larynx, *i.e.*, there was no chance to rotate the probe forward to get any angle for maximum forward position. In this case, the incisors tip, the posterior larynx, and the blade under surface tangent are almost on the same eye-line, *i.e.*, the two eye-line probe representations almost completely overlapped. Again, by mapping the real blade measurements with those extracted from Figure 3(a), we calculate the average value for the view as −0.3 cm. This means that only the back of the larynx is seen, from an approximate distance of 0.3 cm from the beginning of the vocal cords.

Based on the data provided by these experiments (X-ray and photographic records) and by a set of upper airways MR scans from the same subject, a three-dimensional finite element model was set up. Then, a series of different formulations

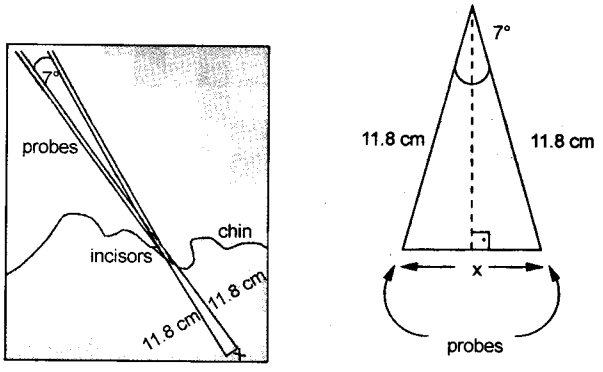

FIGURE 2 Schematic representation based on photographic records of the larynx width and vocal cords view of the patient. The probes measure the angulation values when the vocal cords are still visible and amenable to intubation.

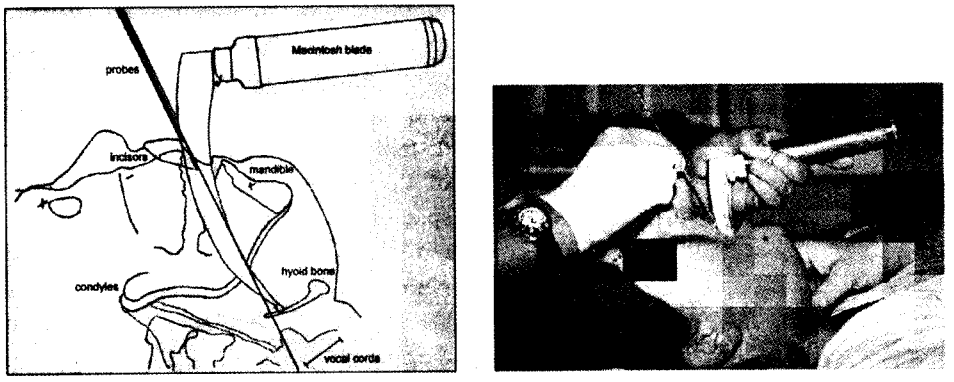

FIGURE 3 Laryngoscopic drawings (a) and photographic records (b) of a laryngoscopy from which data was obtained. The outline drawing was traced from the lateral photograph. The probe is being used as a reference for the measurement of view. The prosthesis attached to the upper incisors has a width of 1.5 cm.

of model parameters were used to simulate deformations of the tongue. To refine and increase the realism of the model, subjective medical feedback was taken into account during the whole modelling process.

3. THE FINITE ELEMENT MODEL OF THE UPPER AIRWAYS

A three-dimensional finite element model of the upper airways of the patient, including the laryngoscope blade, was constructed as shown in Figure 4.

We obtained complete geometric tongue data from MR images and X-ray plates. To simulate mouth opening around the laryngoscope, a 2.5 cm wide plastic device was positioned between the lower and upper incisors of the patient during the scanning session. Once we obtained the tongue data, we converted it into finite elements following the main underlying orientation of the fibres of the tissue [44]. In particular, 280 8-noded bricks were used for representing the tongue structure, tessellating a volume of $6.5 \times 6.0 \times 6.0\,\text{cm}^3$. These brick elements use tri-linear interpolation functions, which allow the study of incompressible and nearly incompressible materials. There are three conventional degrees of freedom associated with each node for this element. There is also one extra node with a single degree of freedom (pressure). This element uses a mixed formulation for incompressible analysis based on the Hermann

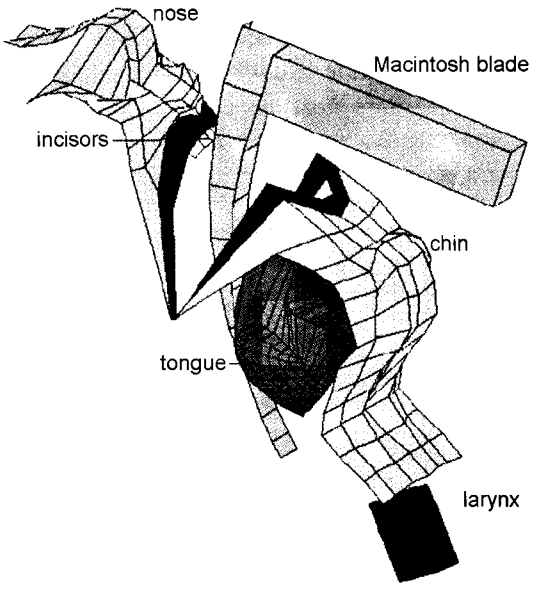

FIGURE 4 Lateral view of the three-dimensional finite element model of the upper airways and the blade during laryngoscopy. Mouth dimensions were extracted from external measurements of the patient, MR images, and X-rays.

formulation, for representing a three-dimensional arbitrarily distorted cube [24].

As to the other components, there are 35 thin shell elements for the blade with data that were obtained from accurate photographs of the laryngoscope with a super-imposed scale to standardize the measurements, and 66 shell elements for the larynx with dimensions that were also extracted from the MR scans. The exact positioning of the larynx during intubation was calculated using the clinical experiments described in Section 2.

In the ideal case, the forces applied by the anaesthetist to the laryngoscope should be directed parallel to the axis of the handle [43]. A few studies have measured and reported the axial forces [1, 3, 4, 13] applied during direct laryngoscopy. The authors of these works used a manufactured laryngoscope handle with strain based sensors to measure force in patients requiring general anaesthesia.

In our model, the laryngoscope is initially positioned forward from the upper incisors and constrained by the size and elastic properties of the tongue. Around the outer periphery of the tongue body, seven axial springs with low stiffness are included into the model and are put into contact with the blade, in order to give shear support, to prevent rigid body motion of the blade, and to avoid geometric collisions between the two structures. The displacement characteristics caused by blade movements are critical and one important consideration is the space into which the tongue volume can be displaced (the soft tissues to the side and below, and the bony constraints, *i.e.*, the mandible).

Following a classical approach, the primary boundary conditions are the forces acting along the dorsum of the tongue (which is essentially pushed down and to the left by the blade), and a set of points in the components that remain fixed, or at least, have restricted movements. The rigid structures (bone attachments) are defined by the nodal points at the front edge and lateral parts of the tongue (attached to the mandible), and the base of skull (condyles) which connects a ligament to the dorsum of the tongue and to the direction of the hyoid bone (shown in Fig. 1) on both sides of the mouth. As shown in Figure 5, fixed displacements in the x, y and z directions (translations and rotations) are set in the area of attachment between tongue and mandible, in the larynx, and at the base of skull. There is no constraint in the middle of the inferior base of the tongue. The hyoid bone area, located along the back end of the basal plane of the tongue, is freely mobile in all directions. There are two boundary conditions applied on the blade surface: one fixed point of rotation on the top, and two face loadings acting on the middle of the blade pushing the tongue down and to the left (not shown in this picture). In particular, the outward normal to the face of the blade determines the positive direction of the load and allows us to apply a distributed load over the face. This load is converted into equivalent nodal loads.

To represent the view of the vocal cords, the distance between the intersection of the tangent

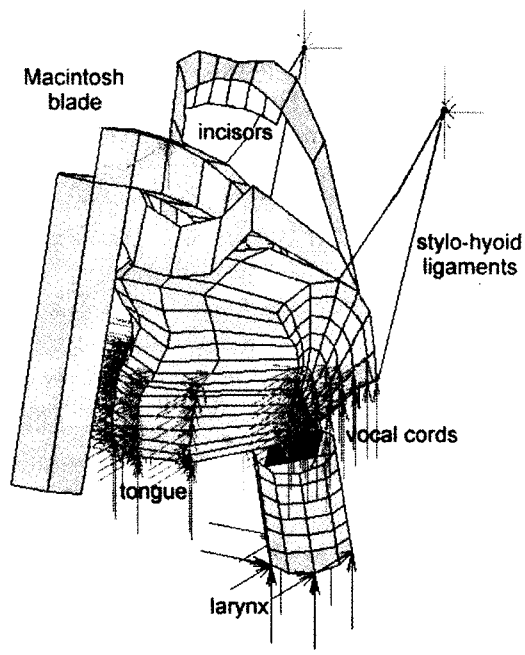

FIGURE 5 The boundary conditions of the model.

with the blade undersurface, and the plane of the cords, and the hyoid point was calculated. The points which define the blade allow exact determination of position and gradient continuously along the curve. This provides an easy and efficient modelling of the vocal cords view by considering the tangents. We have considered the tangent vector at the internal joint between every pair of two consecutive segments and also the tangent vector at the position vectors which belong to the blade undersurface. The limit on anterior rotation of the blade shape occurs when it has maximally compressed the tongue against the buccal surface of the mandible. Posterior rotation of the blade about the hyoid point is limited by contact of the blade incisor surface with the incisor point.

In view of the lack of concrete data for modelling the biological tissue of the tongue, we follow the approach in [6] who found that a good initial approximation for muscle representations can be taken from the properties of rubber materials. The tissue (or muscle) of the tongue is hence assumed to have isotropic elastic properties (meaning that its mechanical properties are the same in all directions), and its volume essentially incompressible. In this case, the *Poisson's ratio* is set to 0.49, a value which represents volume preserving materials. The range of values for the *Young's modulus* spans from 0 up to 14×10^6 dyn/cm^2 which is equivalent to the values of lightly vulcanised rubber [54]. As to the laryngoscopes, they are constructed out of stainless steel with a *Young's modulus* of 1.9×10^{12} dyn/cm^2 and a *Poisson's ratio* of 0.3 [54]. Regarding the specification of the constitutive models to describe the isotropic elastic behaviour of the tongue, we have considered the material models described in the next section.

4. SIMULATING AN EASY CASE OF LARYNGOSCOPY

This section describes the investigation of the soft tissue of the tongue under laryngoscope loading. The analyses use three different material models. The first analysis uses an elastic model; the second model incorporates non-linearities; the third and most complex model incorporates non-linearities and viscoelastic effects. The first two models are rate insensitive, while the others are time-dependent. Basically, we are interested in the deformed shape as a function of the increasing load.

The duration of our laryngoscopic experiments was close to 17 s with a peak force value achieving the best possible view approximately at 11 s. Typical raw data of forces on the tongue [4], and the peak force values collected from different volunteers in experiments done by Bishop *et al.* [1], Bucx *et al.* [4, 3], Hastings *et al.* [13] and McCoy *et al.* [26] were used to generate the loading curves. Figure 6 shows the peak force values for each loading curve. Figure 7 shows a smoothed example of one of those loading curves, as measured by Bucx *et al.* [4]. All the other loading curves are normalised so that the peak force is at 11 s and the total time is 17 s, so that the loading pattern follows that of Figure 7. Although the peak force varied as much as 40 N among curves, all the authors have described the use of similar methods involving subjects with similar anatomical characteristics.

4.1. Linear Elastic Tongue Model

It seems reasonable to approach the problem by using a simple linear model first before going on to large and complicated analyses. In this respect, the tissue of the tongue is described by an isotropic, linear, elastic model which has a linear relationship between stresses and strains.

The view results are displayed in Figure 8. The range of possible solutions indicates loading candidates and stiffness values that may represent the tongue structure according to the empirical solution. In each curve, values smaller than a certain limit for tongue stiffness indicate how the tongue structure eventually collapses, as a function of the respective load that was put onto it. The tongue is deformed beyond certain limits, and

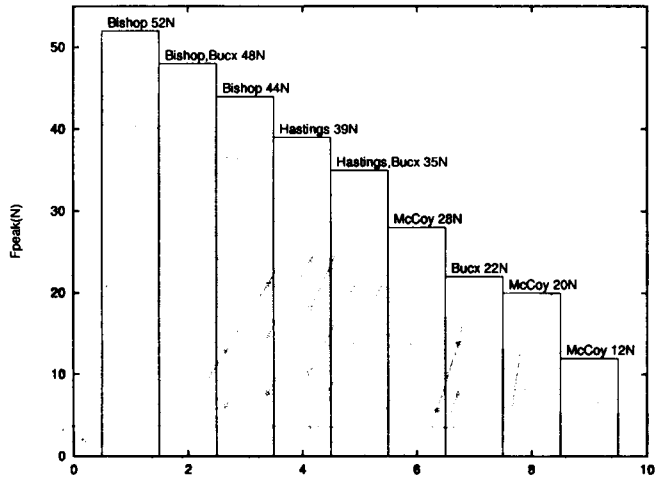

FIGURE 6 Typical peak forces applied during laryngoscopy. Comparisons between their values show quantitative differences, but these are often within the variations arising from different experimental conditions.

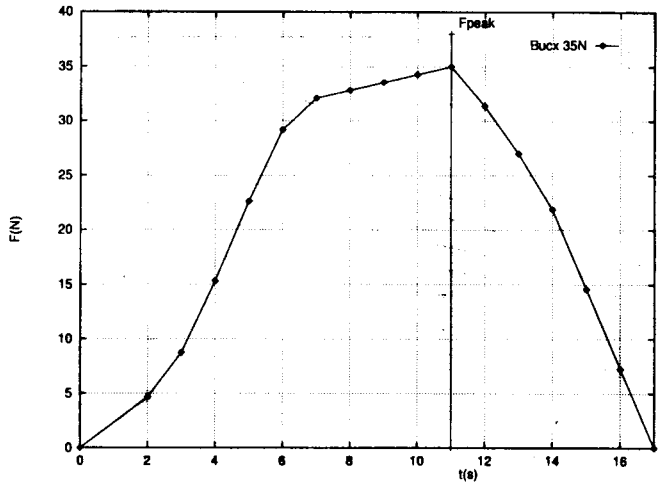

FIGURE 7 A smoothed example of a laryngoscopy loading curve. The nature of the calculation is based on the peak force applied on the tongue, at time = 11 s.

consequently, the view of the cords exceeds a maximal value restrained by the length of the cords and the anterior larynx wall. On the other hand, high stiffness values in some cases impose a restriction on blade movement, and consequently, for tongue deformation, preventing a view of the cords. We assume that the maximal possible stiffness variable for representing the tongue tissue is constrained for values higher than 14×10^6 dyn/cm^2.

Based on the anaesthetist's report which describes the tongue under anaesthesia as being a very soft tissue though each time more difficult to deform, some uncontentious observations can be outlined. For example, from the range of solution of Figure 8, we can say that the linear model allows the inclusion of some relatively stiff material values (such as those close to the soft rubber value of 7×10^6 dyn/cm^2). This seems unlikely due to the softness of the tongue during the procedure. Also,

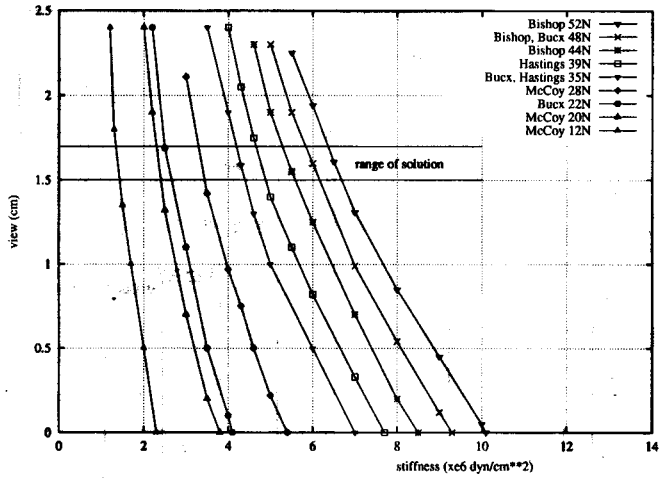

FIGURE 8 The linear tongue model. The diagram shows the loading curves applied to the tongue during the simulation and the different stiffness values chosen for representing the tongue material, plotted against the final view of the cords obtained during the analysis.

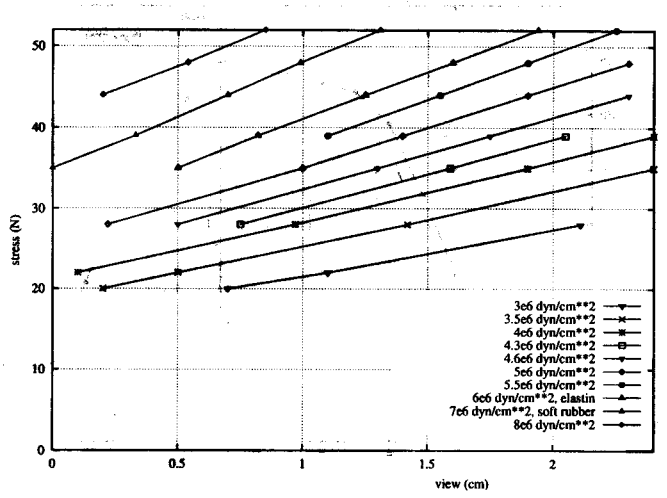

FIGURE 9 The diagram shows, for different stiffness curves, the view plotted against the peak force applied. The linear behaviour of the tongue material is shown.

from Figure 9 this linear tongue behaviour seems to be at variance with the above statement of the anaesthetist who reports an increasing stiffness of the tongue during deformation.

Although this model is a classical way to set a first approximation for the deformation of the soft tissue of the tongue, and is also a simple and inexpensive analysis, other alternative models should be investigated to gain more confidence about the adequacy of the range of solution obtained with the linear model. To this end, more complex behaviours are produced in the following sections by introducing non-linear functions into the model, since for our finite element deformations the non-linear stress–strain characteristics of the living tissues should be accounted for.

4.2. Non-linear Elastic Tongue Model

The tissue of the tongue is represented by a strain-energy function, which characterises the biological tongue muscle showing a non-linear elastic

stress–strain behaviour [41, 42]. The classical Mooney–Rivlin formulation [10, 28] was chosen because it not only provides an accurate representation of the mechanical response for large ranges of deformation [40, 42], but it is also simple enough for setting the material parameters (containing only two material constants) for the analyses.

Figure 10 shows that the non-linear model seems to achieve a more reasonable range (stiffness × view) for representing the tongue. Maximal stiffness values are reduced to values close to the rubber stiffness (8×10^6 dyn/cm^2). Within the range of solution, a stiffness value close to 5×10^6 dyn/cm^2 is the upper limit found. Since the tissue of the tongue is very soft, and even softer under anaesthesia, stiffness values close to the elastin material (6×10^6 dyn/cm^2) [12] or to jelly materials, may be more realistic than those close to the soft rubber material (7×10^6 dyn/cm^2), although there is no empirical evidence for this.

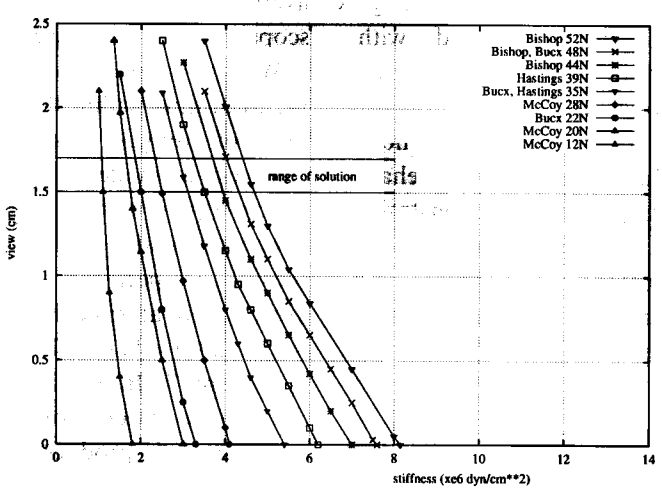

FIGURE 10 The non-linear tongue model. The diagram shows the loading curves applied to the tongue during the simulation and the different stiffness values chosen for representing the tongue material, plotted against the final view of the cords obtained during the analysis.

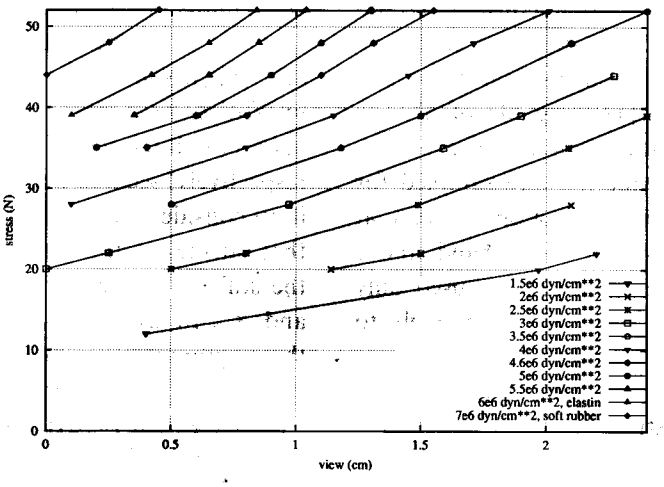

FIGURE 11 The diagram shows, for different stiffness curves, the view plotted against the peak force applied. The non-linear behaviour of the tongue material is shown.

In the non-linear model, at low strains, it is relatively easy to push/dislocate the tongue and the model behaves almost linearly. However, at a particular point of the laryngoscopy, the behaviour of the material becomes stiffer and each time more difficult to deform, even applying higher forces. As previously mentioned, this fact was also confirmed by the anaesthetist when asked to describe subjectively his own perception when trying to push/dislocate the tongue. These observations suggest that the non-linear model provides an improvement over the range of solutions and behaviour obtained with the linear model, and appears to approach actual biological materials more closely.

The next approach is to use the previous non-linear model and introduce more complex behaviour into it by adding viscoelastic constraint functions. A new set of possible solutions can be obtained which may provide more evidence to further constrain the range of possible solutions for the modelling problem.

4.3. Non-linear Viscoelastic Tongue Model

This material corresponds to an extension of the Mooney–Rivlin formulation, in which a time-dependent rate effect of stress is added to represent viscoelastic effects, and in particular, a stress relaxation behaviour. Stress relaxation happens when materials, subjected to a constant strain, relax and the stress gradually decreases with time [33]. We use a fully three-dimensional non-linear viscoelastic formulation [48], capable of accommodating general relaxation times. The relaxation data of our viscoelastic model were sampled for 1 s, 11 s, and 111 s, since extraction of data at values of relaxation times below 1 s and above 111 s are uncertain. These values were used only as trial values to fit the viscoelastic models to our experimental laryngoscopic data.

A recent work published by Hastings *et al.* [13] addresses exactly this stress relaxation phenomenon during laryngoscopy. Although it is still controversial, and does not provide full evidence for the observed facts, the work instigates a more accurate representation of the behaviour of the soft tissues during the blade manoeuvre. The authors report that peak force decreased with time during their laryngoscopic experiments, and in no case did the laryngoscope blade contact the maxillary incisors during the measurement period [14]. However, as far as stress relaxation is concerned, there is no clear evidence about the possibility of establishing a baseline for measuring this phenomenon during the short period (on average, less than 17 s) in which their laryngoscopic experiments were realised.

We are interested in how the vocal cords view varies in time within the inner viscoelastic behaviour of tongue tissue. The time dependent response is modelled by an exponential decay function [48], with a decay factor of 70% of the peak value and a relaxation time of 1,11, and 111 seconds, respectively. Four loading increments are applied at time $t=0$, $t=2.75$, $t=5.50$, $t=8.25$, and $t=11$ s following the loading pattern of Figure 7. In the decay function model, the viscoelastic material of the tongue requires some initial load to produce the deformation at $t=0$, but the load required to maintain this deformation decreases with time.

Figure 12 shows the range of values (stiffness × view) found for representing the model with 11 s of relaxation time. Figure 13 shows the view of the vocal cords plotted against the peak force applied achieved using this model. As the time increases and the tissue of the tongue relaxes, the non-linearities, *i.e.*, the curvature of the stress-view curves (with the relaxation times of 111 s, 11 s, 1 s, respectively) seem to decrease. To be more specific, if we consider the range of possible stiffness values that satisfies all three viscoelastic models, we have the stiffness range composed by the values 5,6,7, and 8×10^6 dyn/cm^2 as a result. By displaying the diagram (view × stress) composed by the three viscoelastic models for one of the above stiffness values, *e.g.*, 7×10^6 dyn/cm^2 (Fig. 14), we can note this fact better. Also, for a same stiffness value the same loading achieves a better view of the cords

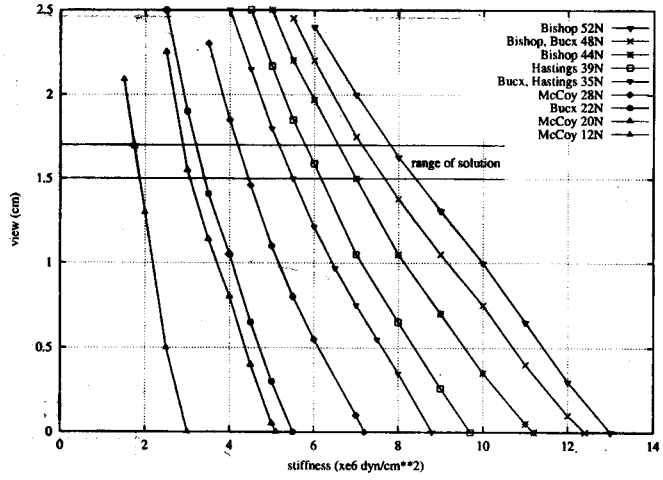

FIGURE 12 The non-linear, viscoelastic tongue model with a relaxation time of 11 s. The diagram shows the loading curves applied to the viscoelastic tongue during the simulation and the different stiffness values chosen for representing the tongue material, plotted against the final view of the cords obtained during the analysis.

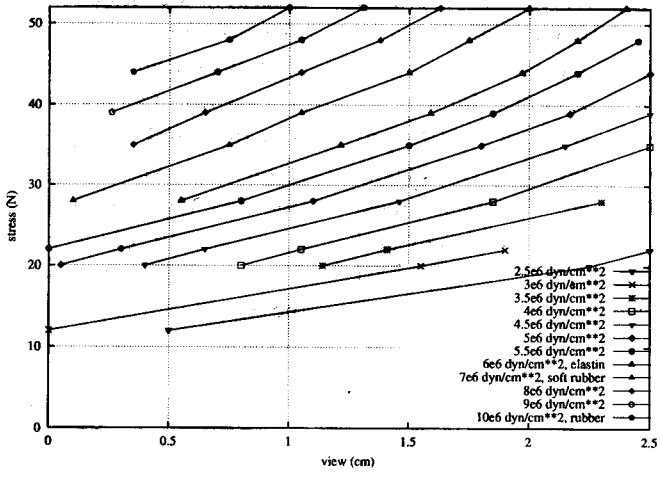

FIGURE 13 The diagram shows, for different stiffness curves, the view plotted against the peak force applied. The non-linear behaviour of the viscoelastic tongue material is shown.

for shorter relaxation times than for longer ones. As an example, in Figure 14, a force of 44 N applied onto the structure of the tongue produces a better view for the viscoelastic material with a relaxation time of 11 s (1.5 cm) than for that of 111 s (0.79 cm).

We observe that if the relaxation time is short compared with the present time, then the stress at a given time becomes small. On the other hand, if the relaxation time is long, then the stress is nearly the same as the original stress. The viscoelastic model with 1 s of relaxation time exhibits a large deformation combined with low stiffness. Because this material deforms very quickly, high stiffness values are needed to prevent the degeneration of the whole tongue structure, and thus, are unlikely to represent the tongue material.

Some general observations suggest that the non-linearities in the behaviour of the models increase according to the following sequence: viscoelastic

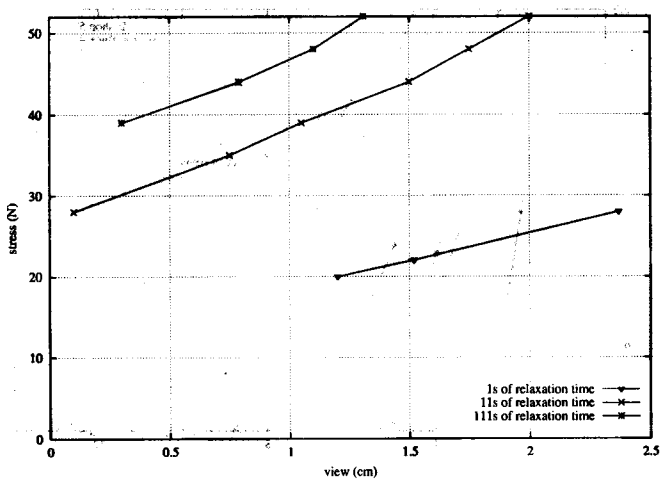

FIGURE 14 Comparisons between the different behaviours of the viscoelastic models with 1, 11, and 111 s of relaxation times, for a stiffness value of 7×10^6 dyn/cm^2.

1 s, viscoelastic 11 s, linear, viscoelastic 111 s, and non-linear models. This behaviour is displayed in Figure 15. Alternatively, we can also investigate how the view improves in each model, for a given load and stiffness value (*e.g.*, 28 N and 4×10^6 dyn/cm^2, respectively). As a result, the viscoelastic models (with 11 s and 111 s of relaxation times) achieve a better view of the cords (1.85 cm and 1.05 cm, respectively), followed by the linear model (0.97 cm), and last, by the non-linear one (0.10 cm). This is shown in Figure 16. In this diagram, we note that the range of possible stiffness values varies significantly among models, even when subject to the same loading (28 N). Apparently, the viscoelastic with 111 s of relaxation time and the linear models produce similar results. The viscoelastic model with 1 s of relaxation time degenerates the tongue structure for the above 4×10^6 dyn/cm^2 stiffness value observed. Finally, we can also compare view values close to the expected solution (1.6 cm) in the easy case, for relatively close stiffness values. This is shown in

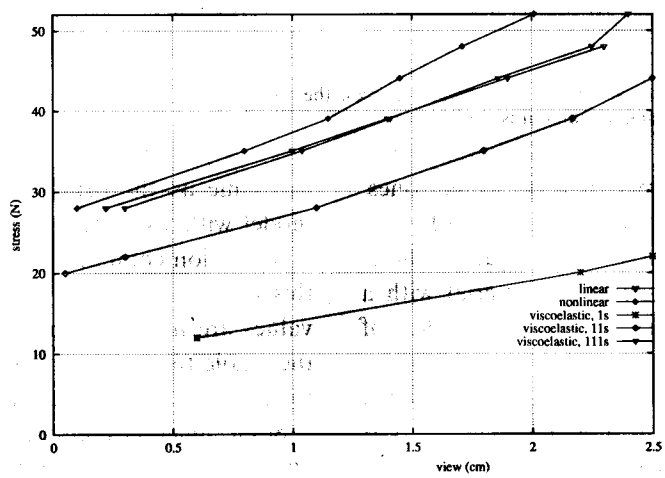

FIGURE 15 The diagram shows the view plotted against the peak force applied, for a stiffness value of 5×10^6 dyn/cm^2. The degree of non-linearities in the curves can be compared.

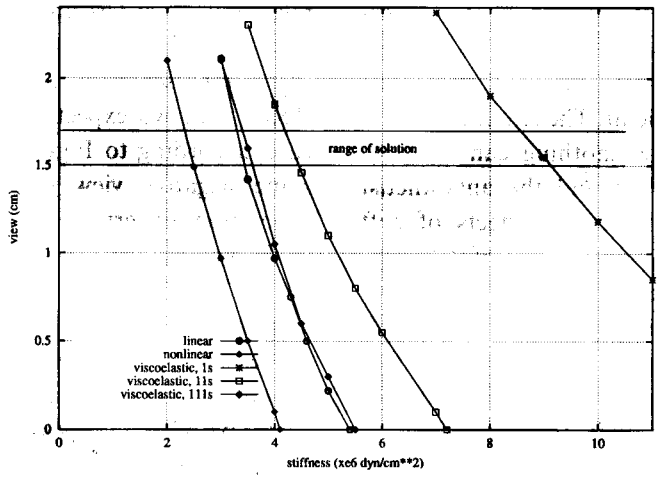

FIGURE 16 The diagram shows the loading curve of 28 N applied to the tongue, with a stiffness value of 4×10^6 dyn/cm^2 plotted against the final view of the cords in each model (linear, non-linear, and all viscoelastic).

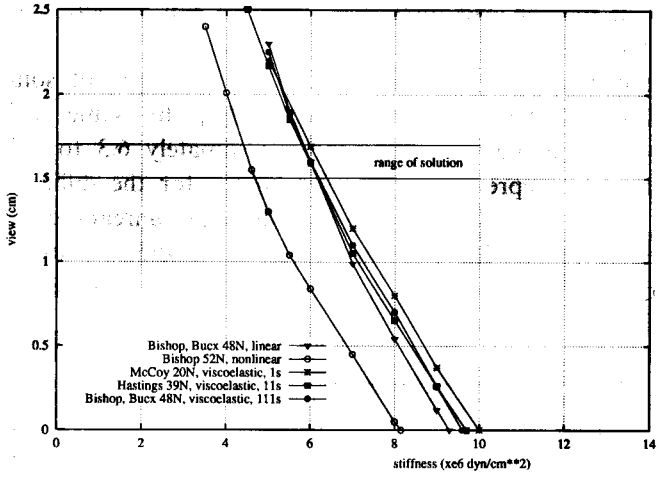

FIGURE 17 The diagram shows possible view solutions where values are close to 1.6 cm, for a same stiffness value.

Figure 17. It is observed that the loading necessary to deform the tongue varies across models and increases in the following order: viscoelastic (1 s, 11 s, 111 s), linear, non-linear.

So far we have dealt with five models to represent the behaviour of the tongue tissue in an easy laryngoscopy experiment. In the next section, we show that the difficult laryngoscopy experiment is also reproducible by applying the same analyses and models utilised in the easy case. In particular, we find a possible range of solutions that satisfies, at a time, both the easy and the difficult experiments.

5. CONSTRAINING THE MODEL PARAMETERS WITH A DIFFICULT CASE

No matter what blade model is used, we suppose that difficult cases need higher force values to achieve a better view of the cords. This seems

reasonable, since the first reaction of the anaesthetist struggling to view the glottis is to increase the effort exerted to dislocate the soft tissues when laryngeal exposure is difficult. The situation can be even worse in cases when nothing can be done about the skeletal problem and the anaesthetist has to cope with the secondary effects of soft tissues (size of the tongue and degree of deformation of the soft tissues, among others).

As reported by the anaesthetist, in the difficult case, the vocal cords could not be seen by him using considerable lifting force with the laryngoscope blade. Assuming that force is inversely related to the laryngeal view, we make use of the top end of Figure 6, which has a peak force value of 52 N. If the top end value is insufficient to displace the tongue, we assume that any other lower values will be insufficient too. On the other hand, if the top end force is excessive and damages the tongue structure, we choose the loading curve with a peak force value immediately below, and so on. Therefore, in a given model, the smaller the loading values, the lower the range of stiffness for representing the tongue tissue.

The results are plotted in Figure 18. We can clearly see that the viscoelastic model with 1 s of relaxation time lies apart from the others in the view domain, and thus, it is excluded as a possible useful representation for the empirical situation. Recall that we expect to obtain no view in this case, according to Figure 3(a) or, more precisely, some negative view close to -0.3 cm. As an estimation of error, we consider the range of probable solutions spanning from 0 to -0.5 cm for the view values.

The remaining models apparently lie within the range of possible solutions in the view domain. However, we need to compare the behaviours of each one of these models in the easy and difficult cases. In this way we can confirm whether, for a specific model, the parameters found as possible solutions in the easy case satisfy also the set of solutions for the difficult case.

The diagram of Figure 18 shows that the linear model is not a good candidate model. Although it achieves a good view value for the cords, within the range of solution for the easy case (Fig. 8), the same stiffness values spanning approximately 6.3 to 6.7×10^6 dyn/cm^2 are not solutions for the difficult case. Moreover, these values are unrealistic because they predict a view in the difficult situation, where we expect to obtain no view at all. Hence, the linear model

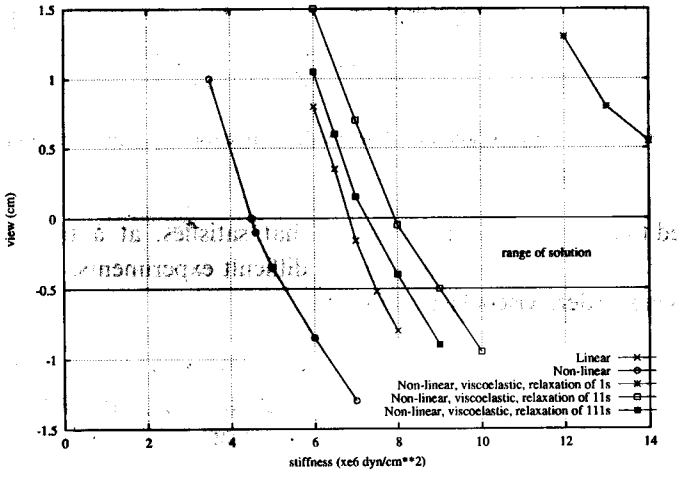

FIGURE 18 A difficult case of laryngoscopy. The diagram shows, for different stiffness curves, the view plotted against the peak force applied.

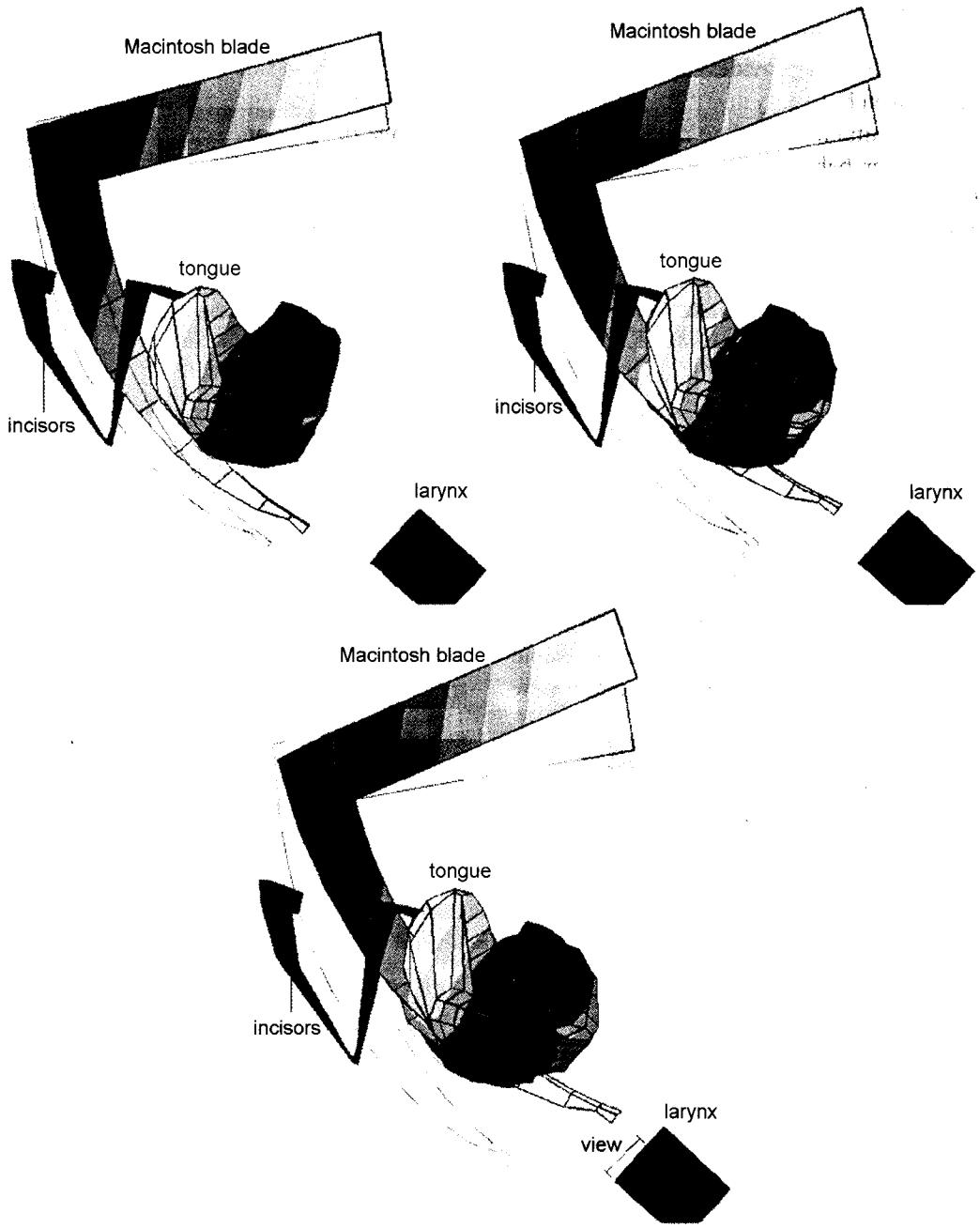

FIGURE 19 Lateral view of a simulated laryngoscopy sequence (easy case) using a laryngoscope blade with 1.59 cm of vocal cords view. This graphic represents the non-linear model, with values of $F_{peak} = 35$ N and tongue stiffness $= 3 \times 10^6$ dyn/cm^2. Changes in stress distribution are represented by the shaded regions (lighter regions correspond to areas of high tensile stresses).

proves itself unsuitable as a possible candidate for representing the behaviour of the tongue during laryngoscopy.

A better behaviour is achieved by the viscoelastic model with 11 s of relaxation time (Fig. 12). It predicts a view using stiffness values spanning

from 7.8 to 8.35×10^6 dyn/cm^2, and no view for values spanning from 7.9 to 9×10^6 dyn/cm^2 (Fig. 18). Therefore, it provides an intersection of solutions between both easy and difficult situations and may be a suitable candidate model.

A much better behaviour is obtained with the non-linear model. It shows a solution range with stiffness values spanning from 4.3 to 4.7×10^6 dyn/cm^2 in the easy case (Fig. 10), and from 4.5 to 5.2×10^6 dyn/cm^2, in the difficult case (Fig. 18). Also, stiffness values that are unrealistic for the easy case are also unrealistic for the difficult case. This fact reinforces the degree of coherency between the parameters used on both laryngoscopic cases, and defines a more refined boundary to further constrain the possible range of solutions. As an example, in Figure 10, a stiffness value of 4×10^6 dyn/cm^2 subject to a loading of 52 N achieves a view of 2 cm in the easy case (beyond the total length of the vocal cords, estimated as 1.80 cm). Not differently, in Figure 18 the same stiffness value used in the easy case achieves a view of 0.5 cm in the difficult situation, whereas no view is expected. Other similar unrealistic values that lack coherency in satisfying both easy and difficult cases at the same time are also considered out of the range of solution.

6. SELECTED SIMULATION SEQUENCES

Illustrative snapshots of the deformations of the tongue are shown in Figures 19–21. We selected 3 out of a sequence of 17 frames to represent the easy case, where the same frame sequence is displayed from three different points of view. The original (only the contour) and the deformed shapes are shown simultaneously. These three-dimensional graphics were selected to convey the scope of some of the possible solutions found using the previous deformable models. In particular, convergent results could be obtained, controlled by a critical evaluation of the geometric

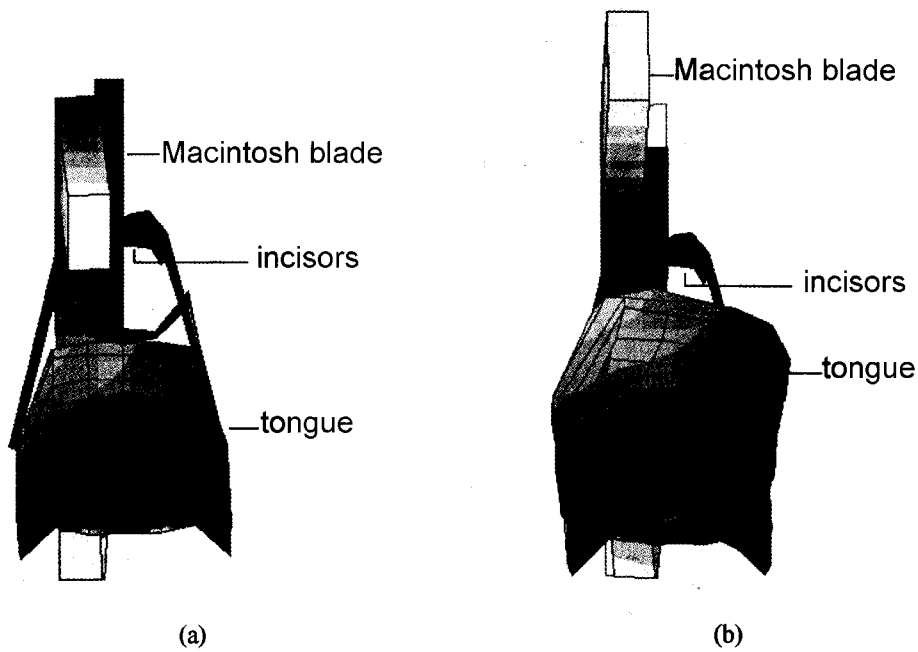

FIGURE 20 Displacement of the tongue to the left (easy case) by a blade. (a) shows the undeformed tongue state, and (b) shows the deformed tongue through a view down the throat towards the tongue. Changes in stress distribution are represented by the shaded regions (lighter regions correspond to areas of high tensile stresses).

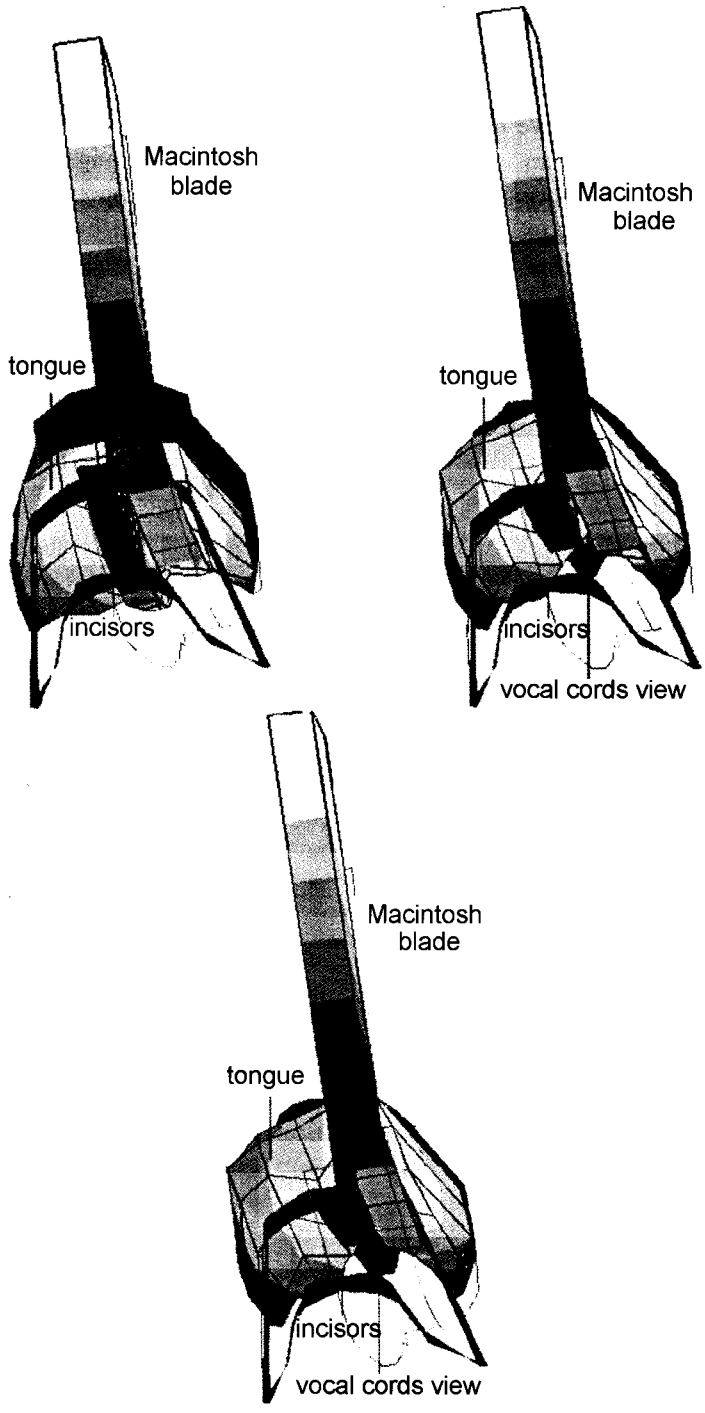

FIGURE 21 In-line view for the easy case. From the left to the right, the original and deformed shapes of tongue and blade are displayed at increments 2,7, and 11, respectively. In the last frame, the tip of the blade is at the mid-line, whereas the left side of the blade at the proximal end (at the lips) is located to the right, very close to the mid-line. Changes in stress distribution are represented by the shaded regions (lighter regions correspond to areas of high tensile stresses).

quality of the tongue mesh, and also of the stress discontinuity between elements during all the analyses. We ran about 800 simulations, each time with a different set of parameters. We believe that we have covered a wide spectrum of possible stiffness values, loadings, and deformable models for representing the soft tissue of the tongue during laryngoscopy. Also, we set a range of parameters for the models in such a way that the corresponding views are biologically plausible with the laryngoscopic experiments.

7. CONCLUSION

Deformable models for simulating laryngoscopy have been proposed and developed successfully. The main upper airway structures have been modelled, providing a simple discrete parametrisation of the tongue, larynx, vocal cords, and blade model during laryngoscopy. External forces applied on the tongue structure were used as the input to the system. By varying the elasticity parameters of the tongue under a given set of conditions, we show that realistic deformations can be achieved, and that both easy and difficult laryngoscopies are reproducible.

The models are based on data obtained from a real patient with a particular interest to simulate the deformation of the tongue, and to observe the consequent view of the vocal cords. In particular, we were able to provide a good three-dimensional tongue mesh from MR images, even using few cross-sections. We have done experiments with five alternative formulations of deformable tongue models. In principle, we used expressions to simulate linear and non-linear elastic materials. The stress relaxation formulation has allowed us to demonstrate interesting viscoelastic effects. A series of finite element analyses were performed to simulate deformations of the tongue; the relationships between the various elastic/non elastic constants were investigated; and a comparison of these simulations with actual deformations was presented.

As regards the behaviour of the models, it is still unclear to what extent a non-linear or viscoelastic model would be the most suitable. In particular, the question arises whether a strain-energy function exists for the tongue material. The existence of a strain-energy function is an assumption that should be justified by experiments analysing the human tongue tissue *in vivo*, consistent with the accepted degree of approximation. Of course, conclusions regarding the validity of the viscoelastic results should be made with caution due to the incompleteness of empirical data concerning the existence of the stress relaxation phenomenon during laryngoscopy. According to our analyses and experiments, the non-linear model behaves similarly to the experimental studies, followed next by the viscoelastic model with 11 s of relaxation time. The ultimate conclusion is certainly linked to empirical studies of tongue tissue and critical analysis of force-feedback systems.

What these experiments do reveal is the kind of investigations involving the material behaviour of the tongue and the vocal cords view. Not all the causes related to the investigation of the outcome of a laryngoscopy were included in this model. However, some important mechanical aspects have been modelled and proved capable of representing realistic information about the complex mechanisms involved. These include the geometry of the upper airways, the deformable behaviour of the tongue and ligaments, and blade shape. Specifically, when the tongue size and elasticity is sufficient to compensate unfavourable factors, such as the geometry, tongue displacement is not difficult; otherwise, difficulty may be anticipated.

These models and simulation prototypes can be used for a number of tasks. These include the formulation of effective strategies for both predicted and unexpectedly difficult laryngoscopy. According to the model configurations, it can also be possible to estimate optimal blade models for patients, and in certain circumstances, predict the occurrence of difficulty. We also believe that computer models of laryngoscopy may be incorporated in simulators for training anaesthetists

and medical students in the future. Finally, we hope that this work can provide the development of a practical but effective graphical, clinical tool for research into the upper airways.

Acknowledgements

The research was partly supported by The National Council for Scientific and Technological Development of Brazil (CNPq) under grant No. 200932/95-0, and by a grant awarded by the British NHS Trust R & D Committee.

References

[1] Bishop, M. J., Harrington, R. and Tencer, A. F. (1992). Force Applied During Tracheal Intubation. *Anesth. Analg.*, **74**, 411–414, The International Anesthesia Research Society.

[2] Bro-Nielsen, M., *Finite Element Modelling in Surgery Simulation*, Technical report, HT Medical Inc., USA, October, 1997.

[3] Bucx, M. J. L., Scheck, P. A. E., Geel, R. T. M., den Ouden, A. H. and Niesing, R. (1992). Measurement of Forces During Laryngoscopy. *Anaesthesia*, **47**, 348–351.

[4] Bucx, M. J. L., Snijders, C. J., van Geel, R. T. M., Robers, C., van Giessen, H., Erdmann, W. and Stijnen, T. (1994). Forces Acting on the Maxillary Incisor Teeth during Laryngoscopy using the Macintosh Laryngoscope. *Anaesthesia*, **49**, 1064–1070.

[5] Charters, P. (1994). Analysis of a Mathematical Model for Osseous Factors in Difficult Intubation. *Canadian Journal of Anaesthesia*, **7**, 594–602.

[6] Chen, D. T. and Zeltzer, D., Pump It Up: Computer Animation of a Biomechanically Based Model of Muscle using the Finite Element Method. *Computer Graphics Proceedings of SIGGRAPH'92, Chicago*, **26**(2), 89–98, July, 1992, ACM Siggraph, Addison Wesley.

[7] Christie, G. W. and Medland, I. C. (1982). A Non-Linear Finite Element Stress Analysis of Bioprosthetic Heart Valves. In: *Finite Elements in Biomechanics*, Ed. by Gallagher, R. H., Simon, B. R., Johnson, P. C. and Gross, J. F., Chichester, U. K., John Wiley & Sons.

[8] Cohen, M. M. and Massaro, D. W. (1993). Modelling Coarticulation in Synthetic Visual Speech. In: Thalmann, D. and Magnenat-Thalmann, N. Editors, *Computer Animation'93*, Springer-Verlag.

[9] Fahy, L., Horton, W. A. and Charters, P. (1990). Factor Analysis in Patients with a History of Failed Tracheal Intubation During Pregnancy. *British Journal of Anaesthesia*, **65**, 813–815, Blackwells Science Publications.

[10] Findley, W. N. and Lai, J. S. Y. (1967). A modified superposition principle applied to creep of nonlinear viscoelastic material under abrupt changes in state of combined stress. *Transactions of the Society of Rheology*, **11**, 361–380.

[11] Fujimura, O. (1977). Model Studies of Tongue Gestures and the Derivation of Vocal Tract Area Functions. In: *Dynamic Aspects of Speech Production*, pp. 225–232, Sawashima, M. and Cooper, F. Eds., Tokyo University Press.

[12] Fung, Y. C. (1993). *Biomechanics – Mechanical Properties of Living Tissues*, Springer-Verlag.

[13] Hastings, R. H., Hon, E. D., Nghiem, C. and Wahrenbrock, E. A. (1996). Force, Torque, and Stress Relaxation with Direct Laryngoscopy. *Anesth. Analg.*, **82**, 456–461, The International Anesthesia Research Society.

[14] Hon, E. D. and Hastings, R. H. (1996). Force, Torque, and Stress Relaxation with Direct Laryngoscopy. *Anesth. Analg.*, In: *Letters to the Editor*, **83**, 1130, The International Anesthesia Research Society.

[15] Janz, R. F., Bruce, R. K. and Moriarty, T. F. (1974). Deformation of the Diastolic Left Ventricle – Part II: Non-Linear Geometric Effects. *J. Biomechanics*, **7**, 509–516.

[16] Janz, R. F. and Grimm, A. F. (1973). Deformation of the Diastolic Left Ventricle – Part I: Non-Linear Elastic Effects. *Biophysics J.*, **13**, 689–704.

[17] Kakita, Y. and Honda, K. (1988). Stability of Vowel Formants Based on a Simple Acoustic Tube Model and a Tongue Model. *Journal of the Acoustical Society of America, Suppl.*, **1**(84), S127.

[18] Kiritani, S., Miyawaki, K., Fujimura, O. and Miller, J. E. (1976). A Computational Model of the Tongue. *Ann. Bull. RILP*, **10**, 243–251.

[19] Koch, R. M., Gross, M. H., Carls, F. R., von Buren, D. F., Fankhauser, G. and Parish, Y. I. H. (1996). Simulating Facial Surgery Using Finite Element Models. *Computer Graphics Proceedings of SIGGRAPH'96*, pp. 421–428, New Orleans.

[20] Ladefoged, P. (1980). Articulary Parameters. *Language and Speech*, **23**, 25–30.

[21] Lee, G. C., Tseng, N. T. and Yuan, Y. M. (1983). Finite Element Modelling of Lungs Including Interlobar Fissures and the Heart Cavity. *J. Biomechanics*, **16**(9), 679–690.

[22] Lee, Y., Terzopoulos, D. and Waters, K. (1995). Realistic Modeling for Facial Animation. *Computer Graphics Proceedings of SIGGRAPH'95*, pp. 55–62, ACM Siggraph, Addison Wesley.

[23] Magnenat-Thalmann, N. and Thalmann, D., The Direction of Synthetic Actors in the Film Rendez-vous à Montréal. *IEEE Computer Graphics and Applications*, pp. 9–19, Dec, 1987.

[24] MARC (1994). *Volume Theory Manual*, MARC Analysis Research Corporation.

[25] Marks, R. R., Hancock, R. and Charters, P. (1993). An Analysis of Laryngoscope Blade Shape and Design: New Criteria for Laryngoscope Evaluation. *Canadian Journal of Anaesthesia*, **40**, 262–270.

[26] McCoy, E. P., Austin, B. A., Mirakhur, R. K. and Wong, K. C. (1995). A New Device for Measuring and Recording the Forces Applied During Laryngoscopy. *Anaesthesia*, **50**, 139–143.

[27] Mermelstein, P. (1973). An Articulatory Model For the Study of Speech Production. *Journal of the Acoustical Society of America*, **53**, 1070–1082.

[28] Mooney, A. (1940). Theory of Large Elastic Deformation. *J. Applied Physics*, **11**, 582–592.

[29] Nahas, M., Hutric, H., Rioux, M. and Domey, J. (1990). Facial Image Synthesis Using Skin Texture Recording. *Visual Computer*, **6**(6), 337–343.

[30] Needleman, A., Rabinowitz, S. A., Bogen, D. K. and McMahon, T. A. (1983). A Finite Element Model of the Infracted Left Ventricle. *J. Biomechanics*, **16**, 45–58.

[31] Oka, M., Tsutsui, K., Ohba, A., Kurauchi, Y. and Tago, T. (1987). Real-Time Manipulation of Texture-Mapped Surfaces. *Computer Graphics Proceedings of SIGGRAPH'87*, **21**, 181–188, ACM Siggraph, Addison Wesley.

[32] Pao, Y. C., Chevalier, P. A., Rodarte, J. R. and Harris, L. D. (1978). Finite Element Analyis of the Strain Variations in Excised Lobe of Canine Lung. *J. Biomechanics*, **11**, 91–100.

[33] Park, J. B. and Lakes, R. S. (1992). *Biomaterials–An Introduction*, Plenum Press, second edition.

[34] Parke, F. (1989). Parameterized Models for Facial Animation Revisited. In: *State of the Art in Facial Animation, SIGGRAPH'89*, Tutorial Notes, pp. 43–56.

[35] Parker, K. J., Gao, L., Lerner, R. M. and Levinson, S. F., Techniques for Elastic Imaging: A Review. *IEEE Engineering in Medicine and Biology*, pp. 52–59, November, 1996.

[36] Pelachaud, C. and Overveld, C. M. A. M. (1994). Modelling and Animating the Human Tongue during Speech Production. *IEEE . Computer Animation'94*, pp. 40–49.

[37] Perkell, J. S., A Physiologically-Oriented Model of Tongue Activity in Speech Production. *Ph.D. Thesis*, Massachusetts Institute of Technology, September, 1974.

[38] Pieper, S., Rosen, J. and Zeltzer, D., Interactive Graphics for Plastic Surgery: A Task-Level Analysis and Implementation. In: *Symposium on Interactive 3D Graphics*, pp. 127–134, Cambridge, Massachusetts, Apr., 1992.

[39] Platt, S. M. and Badler, N. (1981). Animating Facial Expressions. *Computer Graphics Proceedings of SIGGRAPH'81*, **15**(3), 245–252, ACM Siggraph, Addison Wesley.

[40] Rivlin, R. S. (1951). Mechanics of Large Elastic Deformations with Special Reference to Rubber. *Nature*, **167**, 570–595.

[41] Rivlin, R. S. (1997). Some Applications of Elasticity Theory to Rubber Engineering. In: Barenblatt, G. I. and Joseph, D. D. Editors, Collected Papers of R. S. Rivlin, **1**, 9–16, Springer-Verlag, *Proceedings of the Rubber Technology Conference*, London, June, 1948.

[42] Rivlin, R. S. and Sawyers, K. N. (1997). The Strain-Energy Function for Elastomers. In: Barenblatt, G. I. and Joseph, D. D. Editors, Collected Papers of R. S. Rivlin, **1**, 405–417, Springer-Verlag, *Transactions of the Society of Rheology*, **20**(4), 1976.

[43] Roberts, J. T. (1983). *Fundamentals of Tracheal Intubation*, Grune and Stratton.

[44] Rodrigues, M. A. F., Gillies, D. F. and Charters, P., Modelling and Simulation of the Tongue during Laryngoscopy. In: *Computer Networks and ISDN Systems–Special Issue on Visualization and Graphics on the World Wide Web*, **30**(20–21), 2037–2045, Nov., 1998, Extended version of Compugraphics'97 article, Elsevier Science.

[45] Rodrigues, M. A. F., Gillies, D. F., Charters, P. and Marks, R. (1997). Development of a Computer System for Prediction of Difficult Laryngoscopy. *Abstract in the British Journal of Anaesthesia*, **78**, 466–467, Blackwells Science Publications.

[46] Sagar, M. A., Bullivant, D., Mallison, G. D., Hunter, P. J. and Hunter, I. (1994). A Virtual Environment and Model of the Eye for Surgical Simulation. *Computer Graphics Proceedings of SIGGRAPH'94*, pp. 205–212, Orlando.

[47] Scheepers, F., Parent, R. E., Carlson, W. E. and May, S. F. (1997). Anatomy-Based Modeling of the Human Musculature. *Computer Graphics Proceedings of SIGGRAPH'97*, ACM Siggraph, Addison Wesley.

[48] Simo, J. C. (1987). On a Fully Three-dimensional Finite Strain Viscoelastic Damage Model: Formulation and Computational Aspects. *Computer Methods in Applied Mechanics and Engineering*, **60**, 153–173.

[49] Sivarajan, M. and Fink, B. R. (1990). The Position and the State of the Larynx during General Anaesthesia and Muscle Paralysis. *Anesthesiology*, **72**, 439–442.

[50] Stone, M. (1991). Toward a Model of the Three-Dimensional Tongue Movement. *Journal of Phonetics*, **19**, 309–320.

[51] Taber, L. A. (1991). On a Non-Linear Theory for Muscle Shells – Part I: Theoretical Development. *J. Biomech. Engng.*, **113**, 56–62.

[52] Taber, L. A. (1991). On a Non-Linear Theory for Muscle Shells – Part II: Application to the Beating of the Left Ventricle. *J. Biomech. Engng.*, **113**, 63–71.

[53] Terzopoulos, D. and Waters, K. (1990). Physically-Based Facial Modelling, Analysis, and Animation. *Journal of Visualization and Computer Animation*, **1**(2), 73–80.

[54] Timoshenko, G. (1990). *Mechanics of Materials*, PWS-KENT Publishing Company.

[55] Vawter, D. L. (1980). A Finite Element Model for Macroscopic Deformation of the Lung. In: *Finite Elements in Biomechanics*, Ed. by Gallagher, R. H., Simon, B. R., Johnson, P. C. and Gross, J. F., Chichester, U. K., John Wiley & Sons.

[56] Waters, K. (1989). Modelling 3D Facial Expressions: Tutorial Notes. In: *State of the Art in Facial Animation, SIGGRAPH'89*, Tutorial Notes, pp. 127–160.

[57] Wilhelms, J. and Gelder, A. V. (1997). Anatomically Based Modeling. *Computer Graphics Proceedings of SIGGRAPH'97*, pp. 173–180, ACM Siggraph, Addison Wesley.